

Quantifying intermittent transport in cell cytoplasm

Thibault Lagache

Department of Biology, Ecole Normale Supérieure, 46 rue d'Ulm 75005 Paris, France

David Holcman

Department of Mathematics, Weizmann Institute of Science, Rehovot 76100, Israel and
Department of Biology, Ecole Normale Supérieure, 46 rue d'Ulm 75005 Paris, France

Active cellular transport is a fundamental mechanism for protein and vesicle delivery, cell cycle and molecular degradation. Viruses can hijack the transport system and use it to reach the nucleus. Most transport processes consist of intermittent dynamics, where the motion of a particle, such as a virus, alternates between pure Brownian and directed movement along microtubules. In this communication, we estimate the mean time for particle to attach to a microtubule network. This computation leads to a coarse grained equation of the intermittent motion in radial and cylindrical geometries. Finally, by using the degradation activity inside the cytoplasm, we obtain refined asymptotic estimations for the probability and the mean time a virus reaches a small nuclear pore.

Introduction. Cell transport, which may involve vesicles or proteins is essential for cellular function and homeostasis. In general free diffusion in the cell cytoplasm is not efficient and many particles such as large viruses cannot pass the crowded cytoplasm [1] without hijacking the complex cellular transport machinery and use molecular motors, such as dyneins, to travel along microtubules (MTs) toward the nucleus. Both vesicular and viral motions alternate intermittently between periods of free diffusion and directed motion along MTs [2]. Such viral trajectories have been recently monitored by using new imaging techniques *in vivo* [3, 4].

The switch nature of the motion, imposes a complex behavior of the particle trajectories which depends on the number and distribution of MTs, the rate of binding and unbinding and the diffusion constant of the free particle. Some physical properties, such as the mean velocity of trajectories has been obtained for the motion in domain made of parallel strips, in which a random particle has a deterministic motion on the stripes and pure diffusion outside [5]. In case of a population of motors, at equilibrium between free diffusion and bound on MTs, the motor distribution has been studied in cylindrical and radial geometries in [6, 7]; the authors estimate the forward binding rate using Brownian simulations in [6] and experimentally in [7].

We consider here a particle $\mathbf{x}(t)$, which can be described using the stochastic rule:

$$d\mathbf{x} = \begin{cases} \sqrt{2D}d\mathbf{w} & \text{for } \mathbf{x}(t) \text{ free} \\ \mathbf{V} & \text{for } \mathbf{x}(t) \text{ bound} \end{cases} \quad (1)$$

where \mathbf{w} is a standard Brownian motion, D the diffusion constant and \mathbf{V} the velocity of the directed motion along MTs.

In this communication, we compute the mean first passage time of a single particle to a population of MTs. We thus provide an analytical expression of the forward binding rate of a motor to MTs in both radial and cylindrical geometries. Using the analytical expression of the for-

ward binding rate, we propose a coarse-grained description of a switch dynamical motion of a particle, which can either be a virus, a vesicle or a molecular motor. This description, which is the main result of our paper, is a fundamental step to estimate the probability and the mean time to arrive at a small target. Moreover, using this description, we obtain the steady state distribution of virus in MTs network without resorting to the assumption of a two-state model [7, 8].

We thus compute an effective steady state drift $\mathbf{b}(\mathbf{x})$ such that the particle motion (1) can be coarse-grained by the stochastic equation:

$$d\mathbf{x} = \mathbf{b}(\mathbf{x})dt + \sqrt{2D}d\mathbf{w}. \quad (2)$$

Using results derived in [10], equation (2) and the degradation activity in the cytoplasm due to protease or lysosome, we obtain asymptotic estimates of the probability and the mean time for a virus to reach a nuclear pore. The problem of finding a small target is ubiquitous in cellular biology and recent theoretical studies [11, 12] suggest that the geometrical organization of the medium play a fundamental role in this search process.

Mathematical Modeling. We represent the cell cytoplasm as a bounded domain Ω , whose boundary $\partial\Omega$ consists of the external membrane $\partial\Omega_{ext}$ and the nuclear envelope, both of which form a reflecting boundary ∂N_r for the trajectories of (2), except for small nuclear pores ∂N_a , where they are absorbed. The ratio of boundary surface areas satisfies $\varepsilon = \frac{|\partial N_a|}{|\partial\Omega|} \ll 1$. We model the virus degradation activity in the cell cytoplasm as a steady state killing rate $k(\mathbf{x})$ for the trajectories of (2), so the survival probability density function (SPDF) is the solution of the Fokker-Planck equation [13]

$$\begin{aligned} \frac{\partial p}{\partial t} &= D\Delta p - \nabla \cdot \mathbf{b}p - kp \\ p(\mathbf{x}, 0) &= p_i(\mathbf{x}) \end{aligned}$$

with the boundary conditions:

$$p(\mathbf{x}, t) = 0 \text{ on } \partial N_a \text{ and } \mathbf{J}(\mathbf{x}, t) \cdot \mathbf{n}_{\mathbf{x}} = 0 \text{ on } \partial N_r \cup \partial\Omega_{ext} \quad (3)$$

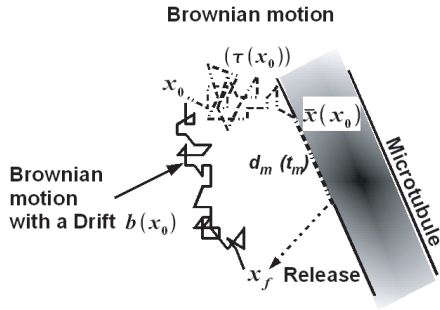


FIG. 1: The fundamental step is represented with a dotted line; a virus starts at a position \mathbf{x}_0 , diffuses freely, binds to a MT over a distance d_m and is then released at a final position \mathbf{x}_f . The solid line represents a trajectory generated by the steady state equation (2). In the parenthesis, we point out the mean times for each portion of trajectories.

where \mathbf{n}_x denotes the normal derivative at a boundary point \mathbf{x} . The flux density vector $\mathbf{J}(\mathbf{x}, t)$ is defined as

$$\mathbf{J}(\mathbf{x}, t) = -D\nabla p(\mathbf{x}, t) + \mathbf{b}(\mathbf{x})p(\mathbf{x}, t). \quad (4)$$

The probability P_N and the mean time τ_N that a trajectory of (2) reaches ∂N_a are given by the small hole theory for two-dimensional domains Ω and drifts $b(x) = -\nabla\Phi(x)$, as [10]

$$\begin{cases} P_N = \frac{\frac{1}{|\partial\Omega|} \int_{\partial\Omega} e^{-\frac{\Phi(\mathbf{x})}{D}} dS_{\mathbf{x}}}{\frac{\ln\left(\frac{1}{\epsilon}\right)}{D\pi} \int_{\Omega} e^{-\frac{\Phi(\mathbf{x})}{D}} k(\mathbf{x}) d\mathbf{x} + \frac{1}{|\partial\Omega|} \int_{\partial\Omega} e^{-\frac{\Phi(\mathbf{x})}{D}} dS_{\mathbf{x}}}, \\ \tau_N = \frac{\frac{\ln\left(\frac{1}{\epsilon}\right)}{D\pi} \int_{\Omega} e^{-\frac{\Phi(\mathbf{x})}{D}} d\mathbf{x}}{\frac{\ln\left(\frac{1}{\epsilon}\right)}{D\pi} \int_{\Omega} e^{-\frac{\Phi(\mathbf{x})}{D}} k(\mathbf{x}) d\mathbf{x} + \frac{1}{|\partial\Omega|} \int_{\partial\Omega} e^{-\frac{\Phi(\mathbf{x})}{D}} dS_{\mathbf{x}}}, \end{cases} \quad (5)$$

Hereafter we derive explicitly the steady state drift $\mathbf{b}(\mathbf{x})$ as a function of some geometrical and dynamical parameters of the cell (number of MTs) and the virus (binding and unbinding rates, the mean velocity \mathbf{V} of the directed motion and the diffusion constant D).

General Methodology. To derive an expression for $\mathbf{b}(\mathbf{x})$, we consider the motion of a virus between the moment it enters the cell at the outer membrane and the moment it reaches the absorbing boundary ∂N_a . Its motion alternates between free diffusion, for a random time τ , until it hits a MT and binds. It continues in a directed motion along the MT for a mean time t_m and a mean distance $d_m = \|\mathbf{V}\|t_m$, until it is released and resumes free diffusion. The steady state drift is chosen to be constant for a sufficiently small step, such that the mean time $\tau + t_m$ to the first release at a point \mathbf{x}_f is the same as that predicted by (2) (see FIG. 1). This approach leads to explicit expressions for the steady state drift for two-dimensional radial and cylindrical geometries.

The steady state drift for a two-dimensional radial cell. We consider a two-dimensional cell cytoplasm which is an annulus Ω of outer radius R and inner radius δ (nuclear surface) with N MTs radially uniformly distributed.

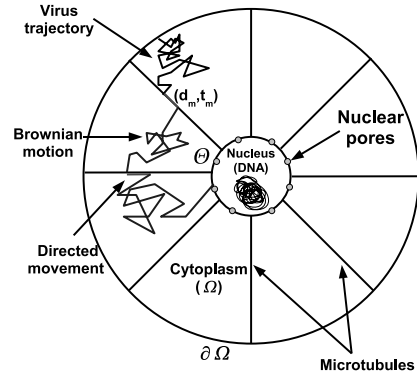


FIG. 2: Two dimensional radial cell with radially equidistributed MTs. We show a virus trajectory alternating between bound and diffusive periods in cytoplasm.

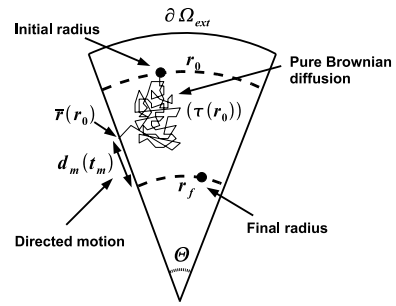


FIG. 3: A fundamental step in $\tilde{\Omega}$. The virus starts at a radius r_0 , with an angle uniformly distributed in $[0; \Theta]$, it diffuses freely during a time $\tau(r_0)$ until it binds to a MT at a mean radius $\bar{r}(r_0)$; it has then a directed motion over a distance $d_m = \|\mathbf{V}\|t_m$ before being released randomly at a final radius r_f . Mean times of each piece of the fundamental step are written inside parenthesis.

They irradiate from the nucleus to the external membrane and the angle between two neighboring ones is $\Theta = \frac{2\pi}{N}$. The two-dimensional approximation applies for culture cells which are flat [14] due to the adhesion to the substrate. In that case the thickness can be neglected in the computation. Before reaching a small nuclear pore, a virus has an intermittent dynamics, alternating between diffusing and bound periods (see FIG. 2). Because the MTs are uniformly distributed, we consider the fundamental domain $\tilde{\Omega}$ defined as the two-dimensional slice of angle Θ between two neighboring ones. In $\tilde{\Omega}$, the fundamental step described above is as follows: the virus starts at a radius r_0 with an angle uniformly distributed in $[0; \Theta]$, it binds to a MT at a time $\tau(r_0)$ and at a radius $\bar{r}(r_0)$. On the MT, it has a radially directed movement towards the nucleus during a mean time t_m and over a distance $d_m = \|\mathbf{V}\|t_m$. Finally, the virus is released with a Θ -uniformly distributed angle at a final radius $r_f = \bar{r}(r_0) - \|\mathbf{V}\|t_m$ (see FIG. 3). In most eukaryotic cell large asters, there are from 600 to 1000 MTs [7]. We can estimate the average number N of MTs per cell cross section as follow: for a cell thickness $h \approx 9\mu\text{m}$,

[7], an interaction range $\gamma \approx 50nm$ between the MTs and the molecular motors [9], and for the AAV diameter $d = 30nm$ [4], we obtain for a radial MT organization in a thin cylindrical cell, that the range of N is between $\frac{600(2\gamma+d)}{h}$ and $\frac{1000(2\gamma+d)}{h}$, that is 9 to 15. We are thus in a regime where $\Theta \ll 1$. For $r_0 < R$, by neglecting the reflecting external boundary at $r = R$, $\tilde{\Omega}$ becomes an open wedge and thus using the standard methods from [15, 16], we obtain

$$\tau(r_0) \approx r_0^2 \frac{\Theta^2}{12D} \text{ and } \bar{r}(r_0) \approx r_0 \left(1 + \frac{\Theta^2}{12}\right). \quad (6)$$

In radial geometry, $\mathbf{b}(\mathbf{x}) = b(r) \frac{\mathbf{r}}{\|\mathbf{r}\|}$ and the MFPT $u(r_0)$ of a virus starting at r_0 and ending at position r_f , described by equation (2) satisfies [17]:

$$D\Delta u - b(r_0)\nabla u = -1 \quad (7)$$

$$\frac{du}{dr}(R) = 0 \text{ and } u(r_f) = 0,$$

where we approximated $b(r)$ by $b(r_0)$. The solution of equation (7) is

$$u(r_0) = \int_{r_f}^{r_0} \left(\int_v^R \frac{ue^{-\frac{b(r_0)}{D}(u-v)}}{Dv} du \right) dv. \quad (8)$$

For $D \ll 1$, using the Laplace method,

$$\int_v^R \frac{ue^{-\frac{b(r_0)}{D}(u-v)}}{Dv} du \approx \frac{1}{b(r_0)}. \quad (9)$$

Thus, in first approximation, $u(r_0) \approx \frac{r_0 - r_f}{b(r_0)}$. To obtain the value $b(r_0)$, we equal the MFPT $u(r_0)$ from r_0 to r_f computed from equation (2) with the one obtained from an intermittent dynamic: $\tau(r_0) + t_m$. Consequently, we get:

$$b(r_0) = \frac{r_0 - r_f}{\tau(r_0) + t_m} = \frac{d_m - r_0 \frac{\Theta^2}{12}}{t_m + r_0^2 \frac{\Theta^2}{12D}}. \quad (10)$$

Tests against Brownian simulations. We impose reflecting boundaries at the external membrane $r = R$ and we tested the theoretical steady state distribution against the one obtained by running empirical intermittent Brownian trajectories in the pie wedge domain. For a potential field, the steady state distribution satisfies $D\Delta p - \nabla[\mathbf{b}p] = 0$ in Ω with reflecting boundary condition $\mathbf{J}(\mathbf{x}, t) \cdot \mathbf{n}_x = 0$ on $\partial\Omega$. The distribution p in a two-dimensional radial geometry is:

$$p(r) = \frac{e^{-\frac{\Phi(r)}{D}}}{\int_0^R e^{-\frac{\Phi(r)}{D}} 2\pi r dr}, \quad (11)$$

which should be compared to the distribution of [7]. The potential Φ of $b = -\nabla\Phi$ is obtained by integrating equation (10) with respect to r ,

$$\Phi(r) = \frac{d_m \sqrt{12Dt_m}}{t_m \Theta} \arctan\left(\frac{\Theta r}{\sqrt{12Dt_m}}\right) - \frac{D}{2} \ln(12Dt_m + r^2\Theta^2) \quad (12)$$

Steady State Distribution

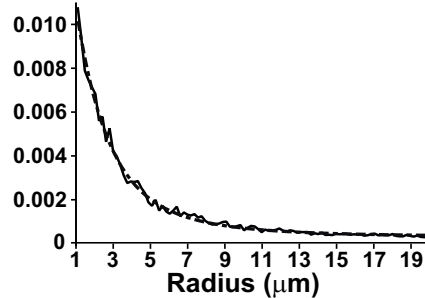


FIG. 4: Steady state distributions. Dashed line: virus distribution (11) with the effective drift $b(r)$ (10); solid line: Empirical steady state distribution obtained by running 10,000 intermittent Brownian trajectories. The cell radius is $R = 20\mu m$ and $\Theta = \frac{\pi}{6}$.

In FIG. 4, we plotted the steady state distribution given in (11) against the distribution obtained by the intermittent empirical equation (1). The parameters are chosen such that the viruses move towards the nucleus (observed *in vitro*, loaded dynein moves during 1s over a distance of $0.7\mu m$ [18]), we thus take $t_m = 1s$ and $d_m = 0.7\mu m$; furthermore, the diffusion constant is $D = 1.3\mu m^2 s^{-1}$ as observed for the Associated-Adeno-Virus [4]. The nice agreement of both curves, which is the central result of this communication, confirms that our coarse grained method accounts well for the switch system (1).

Computation of P_N and τ_N . We derive now asymptotic expressions in the small diffusion limit $D \ll 1$, for the probability P_N and the mean time τ_N a virus arrives at a small nuclear pore. We apply Laplace's method in formulas (5) for a radial geometry. When the degradation rate $k(r)$ is taken constant, equal to k_0 in the neighborhood of the nucleus $r = \delta$ and when $12d_m > r\Theta^2$, $b(r) > 0$ so that Φ reaches its minimum at $r = \delta$, we get

$$P_N = \frac{b(\delta)}{\ln\left(\frac{1}{\epsilon}\right) 2\delta k_0 + b(\delta)} \text{ and } \tau_N = \frac{\ln\left(\frac{1}{\epsilon}\right) 2\delta}{\ln\left(\frac{1}{\epsilon}\right) 2\delta k_0 + b(\delta)}.$$

A Taylor expansion for $\Theta \ll 1$ gives that

$$P_N \approx \frac{d_m}{d_m + K} \left(1 - \frac{K\delta(d_m\delta + Dt_m)}{12Dt_m d_m(d_m + K)} \Theta^2\right) \quad (13)$$

$$\tau_N \approx \frac{K}{k(d_m + K)} \left(1 + \frac{\delta(d_m\delta + Dt_m)}{12Dt_m(d_m + K)} \Theta^2\right) \quad (14)$$

where $K = 2k_0\delta t_m \ln\left(\frac{1}{\epsilon}\right)$.

We can now propose the following predictions: because nuclear pores occupy a fraction $\epsilon = 2\%$ [19] of the nucleus surface (radius $\delta = 8\mu m$) and the measured degradation rate for plasmids [20] is $k = \frac{1}{3600} s^{-1}$, we obtain from formula 13-14 that

$$P_N \approx 94.3\%, \tau_N \approx 205s. \quad (15)$$

We conclude that the infection efficiency is very high, while the mean time to reach a nuclear pore is of the

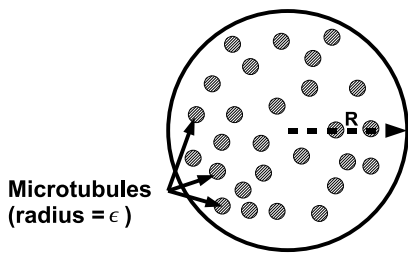


FIG. 5: Dendrite cross-section. The N MTs are thin cylinders uniformly distributed inside the dendrite.

order of 3 minutes. It is interesting to compare this time with the 15 minutes reported in [4], which accounts for all the viral infection steps from the entry to the final nuclear import. This difference between the two times indicates that the phase where the virus is inside an early endosome (EE) may last 10 minutes. Indeed, the endosomal phase ends once the EE has matured into a late endosome (LE) [21], which lasts approximately 10 minutes [22]. To finish, we shall note that a free diffusing virus would reach a nuclear pore in about 15 minutes [11].

The cylindrical geometry. Many transports mechanisms such as viral (herpes virus [23]) and vesicular occur in long axons or dendrites, which can be approximated as thin cylinders (radius R and length L). To derive a quantitative analysis of viral infection in that case, we follow the method described above and compute the steady state drift that accounts for the directed motion along MTs. We model the N MTs parallel to the dendrite principal axis as cylinders (radius $\epsilon \ll R$, Length L). The cross-section Ω of the dendrite is shown in FIG. 5. Due to the cylindrical symmetry, for any position \mathbf{x} , the steady state drift $\mathbf{b}(\mathbf{x})$ is equal to $B\mathbf{z}$ where B is a constant and \mathbf{z} the principal axis unit vector along the dendrite. In a small diffusion approximation, the leading order term of B is equal to the effective velocity [5, 6]: $B = \frac{d_m}{t_m + \tau}$, where t_m is the mean time the virus binds to a MT,

$d_m = \|\mathbf{V}\|t_m$ the mean distance of a run and τ the MFPT to a MT. To derive an expression for τ , we consider the cross-section Ω and impose reflecting boundary condition at the external membrane of the dendrite ($r = R$) and absorbing ones at the MTs surfaces. In long time approximation, for a MTs radius $\epsilon \ll 1$, τ is asymptotically equal to $\frac{1}{\lambda D}$ where λ is the first eigenvalue of the Laplace operator in Ω with the boundaries conditions described above ([17] p.175). The leading order term of λ as a function of ϵ is [24] $\lambda = \frac{2\pi N}{|\Omega| \ln(\frac{1}{\epsilon})}$, where $|\Omega| = \pi R^2$.

Thus, the MFPT to a MT is $\tau = \frac{1}{\lambda D} = \frac{R^2 \ln(\frac{1}{\epsilon})}{2ND}$, and the steady state drift amplitude B is given by

$$B = \frac{d_m}{t_m + \tau} = \frac{2NDd_m}{2NDt_m + R^2 \ln(\frac{1}{\epsilon})}. \quad (16)$$

We conclude that in the limit $t_m \ll \tau$, the effective velocity is proportional to the number of MTs: $B \approx N \frac{2Dd_m}{R^2 \ln(\frac{1}{\epsilon})}$, as already observed in [7].

Conclusion. Intermittent dynamics with alternative periods of free diffusion and directed motion along MTs characterizes many cellular transports. We have developed a model to estimate a steady state drift such that the intermittent dynamic can be described by an over-damped limit of the Langevin equation. Our method gives explicit results in two-dimensional radial cell and in a cylindrical dendrite or axon. The steady state description of the movement enables us to estimate the probability a virus reaches alive a small nuclear pore and its mean time. Because viruses are very efficient DNA carriers, understanding and quantifying their movement in the cell cytoplasm would be very helpful for designing synthetic vectors [25]. In a future work, it would be interesting to derive steady state drifts for three dimensional geometries.

Acknowledgments: D. H. research is partially supported by the program ERC-starting Grant.

-
- [1] B. Sodeik, Trends Microbiol. **8**, 465 (2000).
[2] U.F. Greber, Cell. **124**, 741 (2006).
[3] N. Arhel et al., Nature Methods **3**, 817 (2006).
[4] G. Seisengerger et al., Science **294**, 1929 (2001).
[5] A. Ajdari, Europhys. Lett. **31**, 69 (1995).
[6] R. Lipowsky, S. Klumpp and T.M. Nieuwenhuizen, Phys. Rev. Lett. **87**, 108101 (2001).
[7] F. Nedelec, T. Surrey and A.C. Maggs, Phys Rev Lett. **86**, 3192 (2001).
[8] S. Klumpp, T.M. Nieuwenhuizen and R. Lipowsky, Biophys. J. **88**, 3118 (2005).
[9] D. Coy, M. Vagenbach and J.J. Howard, Biol. Chem. **274**, 3667 (1999).
[10] D. Holcman, Journ. of Stat. Phys. **127**, 471 (2007).
[11] Z. Schuss, A. Singer and D. Holcman, Proc. Natl. Acad. Sci. U.S.A. **104**, 16098 (2007).
[12] S. Condamin et al., Nature **450**, 77 (2007).
[13] D. Holcman, A. Marchewka and Z. Schuss, Phys. Rev. E **72**, 031910 (2005).
[14] A.T. Dinh et al. Biophys J. **89**, 1574 (2005).
[15] S. Redner, *A Guide to First-Passage Processes*(Cambridge University Press, Cambridge, 2001).
[16] T. Lagache and D. Holcman (to be published).
[17] Z. Schuss, *Theory and Applications of Stochastic Differential Equations* (John Wiley, New York, 1980).
[18] S.J. King, T.A. Schroer, Nat. Cell Biol. **2**, 20 (2000).
[19] G. Maul and L. Deaven, J. Cell Biol. **73**, 748 (1977).
[20] D. Lechardeur et al., Gene Therapy **6**, 482 (1999).
[21] W. Ding et al., Gene Therapy **12**, 873 (2005).
[22] J. Rink et al., Cell **122**, 735 (2005).
[23] G.A. Smith et al., Proc. Natl. Acad. Sci. U.S.A. **45**, 16034 (2004).
[24] S. Ozawa, Proc. Japan. Acad. **56**, 459 (1980).
[25] G. Zuber et al., Adv Drug Deliv Rev. **52**, 245 (2001).